TOXICOLOGICAL SCIENCES **84**, 110–119 (2005)
doi:10.1093/toxsci/kfi052
Advance Access publication December 8, 2004

In Vitro Zonation and Toxicity in a Hepatocyte Bioreactor

Jared W. Allen, Salman R. Khetani, and Sangeeta N. Bhatia[1]

Departments of Bioengineering and Medicine, University of California at San Diego, La Jolla, California 92093-0412

Received July 8, 2004; accepted December 4, 2004

The complex architecture of the liver is intertwined with its response to xenobiotic compounds. In particular, hepatocyte subpopulations are distributed along the sinusoid in zones 1 to 3, leading to prototypical "periportal" and "centrilobular" patterns of cell death in response to a toxic insult. *In vitro* models that more closely represent these zones of sub-specialization may therefore be valuable for the investigation of hepatic physiology and pathophysiology. We have established a perfused hepatocyte bioreactor that imposes physiologic oxygen gradients on co-cultures of rat hepatocytes and non-parenchymal cells, thereby producing an *in vitro* model of zonation. In order to predict and control oxygen gradients, oxygen transport in a parallel-plate bioreactor containing co-cultures was first mathematically modeled and experimentally validated. Co-cultures exposed to these physiologic oxygen gradients demonstrated regionally heterogeneity of CYP2B and CYP3A protein that mimics the distribution seen in the zonated liver. The distribution of CYP expression in the bioreactor was shown to vary with exposure to different chemical inducers and growth factors, providing a potential platform to study physiologic zonal responses. In order to explore zonal hepatotoxicity, bioreactors were perfused with APAP (acetominophen) for 24 h, resulting in maximal cell death at the low-oxygen outlet region similar to centrilobular necrotic patterns observed *in vivo*. This hepatocyte bioreactor system enables further *in vitro* investigation into zonation-dependent phenomena involving drug metabolism and toxicity.

***Key Words:* *in vitro* models; liver zonation; acetaminophen; cytochrome P450 induction; hepatocyte bioreactor; centrilobular.**

The liver is a major site for xenobiotic metabolism and biotransformation. *In vitro* models of the liver have played a critical role in advancing our understanding of drug metabolism, their mechanisms of action, and potential deleterious effects. However, current *in vitro* models offer a relatively homogeneous view of liver function when, in fact, the morphology and function of hepatocytes are known to vary with position along the liver sinusoids from the portal triad to the central vein. This phenomenon, known as zonation, has been described in virtually all areas of liver function. Oxidative energy metabolism, carbohydrate metabolism, lipid metabolism, nitrogen metabolism, bile conjugation, and xenobiotic metabolism have all been localized to separate zones. Such compartmentalization of gene expression is thought to underlie the liver's ability to operate as a ''glucostat'' as well as the pattern of zonal hepatotoxicity observed with some xenobiotics (e.g., acetominophen) and environmental agents (e.g., carbon tetrachloride). The distribution of functions along the sinusoid is thought to be modulated by diverse factors such as oxygen and hormone gradients, nutrients, matrix composition, and even the distribution of non-parenchymal cells (Jungermann and Kietzmann, 1996; Jungermann and Thurman, 1992; Lindros, 1997). However, *in vitro* models that incorporate variations in of the liver microenvironment along the sinusoid in order to induce and study zonation-dependent phenomena are limited.

The gold standard for investigation of zonal responses is immunohistochemical staining of tissue sections (Baron *et al*., 1982; Giffin *et al*., 1993). This destructive technique is limited due to animal-to-animal variability and necessarily complicates the investigation of time-dependent phenomena. Other methods include attempts to isolate sub-populations from the liver with microdissection or zone-specific hepatocyte isolation, *ex vivo* whole organ perfusion (Bars *et al*., 1992; Haussinger, 1983; Teutsch, 1986). Alternatively, mixed populations of hepatocytes have been isolated and ''induced'' to compartmentalize in culture by environmental cues (Kietzmann *et al*., 1999). Oxygen, in particular, has been shown to play an important role in modulation of zonal gene expression in hepatocyte cultures (Jungermann and Kietzmann, 2000); however, liver-specific gene expression rapidly declines in monolayer culture limiting the utility of such models. Furthermore, existing models do not account for the interaction between hepatocyte subpopulations through a fluid conduit as exists in the liver. Continuously-perfused bioreactors combined with phenotypically stable hepatocyte cultures may offer the ability to (1) induce compartmentalization of mixed cultures through control of the local oxygen concentration, (2) allow exchange of paracrine signals between zonal subpopulations, and (3) study the dynamics and consequences of zonation.

Thus, in effort to recapture the zonal features of the liver, we have developed a biomimetic flat-plate bioreactor system housing phenotypically stabilized hepatocyte-fibroblast co-culture. Mathematical modeling of oxygen transport, coupled with

[1] To whom correspondence should be addressed at Harvard-MIT Division of Health Sciences and Technology (HST)/Electrical Engineering and Computer Science, MIT, 77 Massachusetts Ave., Bldg E19, 5th floor, Cambridge, MA 02139. E-mail: sbhatia@mit.edu.

experimental validation of steady-state oxygen gradients allowed initial characterization and optimization of operational parameters. Using this perfusion system, we examined the role of oxygen and nutrient gradients on the spatial induction of CYP2B and CYP3A. Furthermore, the toxicity of acetaminophen (APAP) under perfusion conditions and physiologic oxygen gradients was evaluated.

MATERIALS AND METHODS

Hepatocyte isolation and culture. Primary rat hepatocytes were isolated and purified by a modified procedure of Seglen (Seglen, 1976). Briefly, 2–3 month old adult female Lewis rats (Charles River Laboratories, Wilmington, MA) weighing 180–200 g were anesthetized prior to *in situ* perfusion of the portal vein. Following a two-step perfusion of Krebs Ringer Buffer and collagenase, dissociated cells were passed through nylon mesh and purified on a Percoll gradient. Prior to seeding, microscope slides (38 × 75 mm) were washed in ethanol, rinsed thoroughly with sterile water, and incubated for 1 h at 37°C in a type I collagen solution (0.05 mg/ml). Following collagen adsorbsion, 1.5 × 106 hepatocytes were seeded on each slide and allowed to attach for 2 h, at which point media was replaced. Co-cultures were created by adding 750,000 J2-3T3 fibroblasts/slide 24 h after hepatocyte seeding (Bhatia *et al*., 1999). Similar co-cultures and hepatocyte only cultures were created in six-well plates with hepatocyte and fibroblast concentrations of 250K and 125K, respectively. Bioreactor cultures were allowed to stabilize to day 5 with media changes every 48 h. Hepatocyte co-cultures were maintained in Dulbecco's Modified Eagle Medium (DMEM, GibcoBRL, Rockville, MD) with 10% fetal bovine serum, supplemented with insulin, hydrocortisone, and antibiotics and fibroblasts in DMEM with 10% FBS. All cultures were buffered using sodium bicarbonate and 5% CO_2.

Bioreactor and flow circuit. The flat-plate bioreactor designed to house hepatocyte cultures on 38 × 75 mm microscope slides was described previously, though system optimizations are mentioned here (Allen and Bhatia, 2003). Between days 5–7 post-isolation, co-cultures were sealed in chamber blocks fabricated from polysulfone which facilitate sterilization needed for long term perfusion. After assembly, the chamber was inserted to the flow circuit (Fig. 1) containing a media reservoir, gas exchanger, O_2 probe, and syringe pump. Pressure-driven flow was continuous using a programmable push-pull syringe pump (Harvard Apparatus). Media was equilibrated with a mixture of 10% O_2, 5% CO_2, 85% nitrogen in a gas exchanger made with gas permeable silastic tubing. Outlet oxygen measurements were recorded using a miniature Clark-type electrode (Microelectrodes, Inc, Bedford, NH). Electrode zeroing was carried out periodically while calibration at the inlet pO_2 was carried out prior to each experiment. Experimental flow rates of recirculating media varied from 0.2 ml/min to 4 ml/min. All flow circuit components except for the syringe pump were housed in a PID-controlled incubator maintained at 37°C.

Hepatocyte induction and toxicity. Bioreactor cultures and conventional cultures were incubated with media supplemented with various drugs to evaluate regional changes in protein expression and toxicity. Induction of CYP2B and CYP3A was carried out by adding 200 μM phenobarbital (PB) or 5 μM dexamethasone (DEX), respectively. Additionally, epidermal growth factor (EGF) was added at a concentration of 2 nM to examine its role in modulating CYP expression. Drug exposure was initiated between days 5–7 post-isolation for all cultures and was maintained for 48 h. Toxicity experiments for both static and perfused cultures were performed by adding APAP ranging from 5–40 mM to culture media for 24 h.

Viability assay. Viability of perfused cultures was determined using fluorescence by 30-min incubation of calcein AM (viable – ex494/em516) and ethidium homodimer (non-viable – ex528/em617) (Molecular Probes) followed by 1 min incubation of 0.01% Hoechst dye 33258 (nuclear – ex365/em458). In toxicity studies, cultures were incubated with 0.5 mg/ml thiazolyl blue (MTT) in DMEM for 3 h after treatment. Formazan formation was quantified by extracting the precipitate with a 1:1 mixture of dimethyl sulfoxide and isopropyl alcohol and measure absorbance at 570 nm.

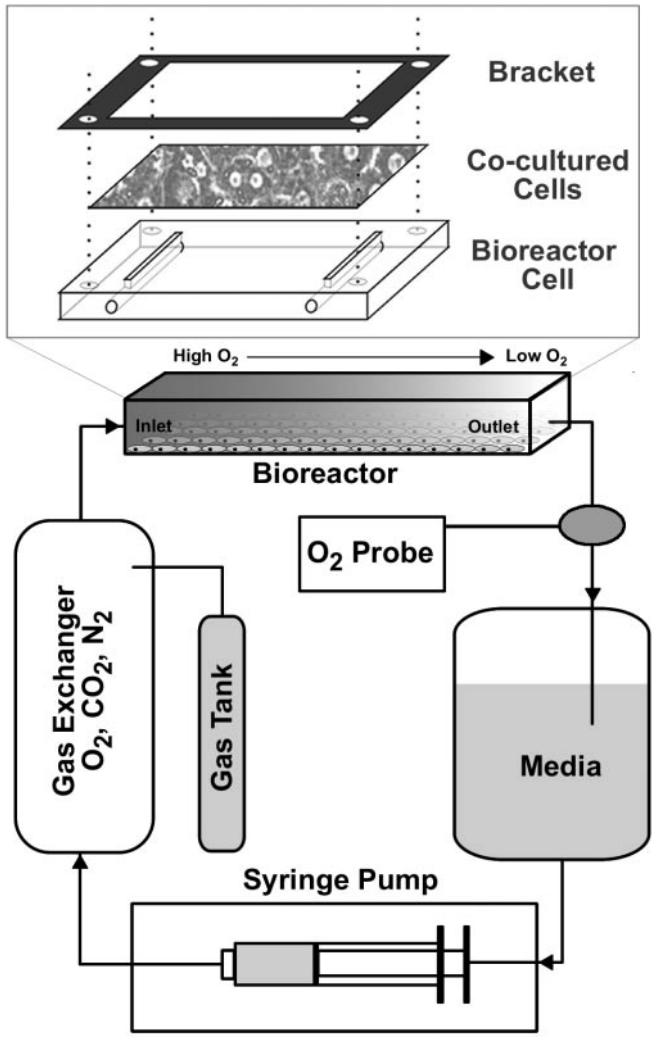

FIG. 1. Bioreactor design and circuit. Experiments were carried out with a perfusion circuit and flat-plate bioreactor as indicated. All components except the syringe pump were maintained at 37°C.

Microscopy and image analysis. Images were obtained using a Nikon Eclipse TE300 inverted microscope, CCD camera (CoolSnap HQ, Roper Scientific), and Metamorph Image Analysis System (Universal Imaging). Percent viability in cultures treated with fluorescent viability markers was determined by counting the number of dead cells relative to total cells. In each case, images were acquired in triplicate from inlet, midline, and outlet regions of the slide. Evaluation of MTT-stained cultures was carried out by obtaining full-field images using a Nikon Coolpix 3100 digital camera and also a series low-magnification images from the Nikon TE200. Relative viability was determined from the optical density of triplicate images at five positions along the length of the slide.

Western blot analysis. Cultures from chamber slides were lysed and scraped in Ripa lysis buffer (Upstate, Waltham, MA) supplemented with Complete protease inhibitor cocktail (Roche Diagnostics, Indianapolis, IN). Samples were homogenized with a pestle, and centrifuged at 16,200 × *g* for 5 min. Total protein content in the supernatant was determined using the DC protein assay (Bio-Rad, Hercules, CA) and used to normalized sample loading.

Samples prepared in sample buffer were loaded (20 μg/well) for electrophoresis on a 10% polyacrylamide gel. After overnight transfer on to a PVDF membrane, blots were incubated with a blocking buffer (20 mM Tris/HCl [pH 7.4], 500 mM NaCl, 0.1% Tween 20, and 5% [w/v] milk powder) and washed with buffer without milk powder. Incubation for 1 h with primary antibody against rat CYP2B or CYP3A (Gentest, Woburn, MA) was followed by washing and incubation with either anti-goat (CYP2B) or anti-rabbit (CYP3A) HRP-conjugated secondary antibody for 45 min. After washing, the Pierce SuperSignal chemiluminescence reagent was used for detection. All electrophoresis gels were run with molecular weight markers to verify CYP bands (~56 kDa).

Statistics and data analysis. Statistical analysis and model computations were performed using Mathcad (Mathsoft, Inc. Cambridge, MA), which provides a symbolic interface for evaluating the analytical solution or Matlab (Mathworks, Inc., Natick, MA) for analysis of the numerical solution. Model and experimental data were plotted using Sigmaplot (SPSS, Inc., San Rafaael, CA). Error was reported at the standard error of the mean and statistical significance was determined using one-way ANOVA ($p < 0.05$).

Mathematical modeling. The model of transport of oxygen in the parallel-plate bioreactor was described previously. Briefly, beginning with the equation of continuity for a binary system and assuming steady-state transport in a uniform flow field in the x direction and lateral diffusion in the y direction, the non-dimensional governing equation and boundary conditions are obtained (Equations 1–4):

$$\frac{\partial \hat{c}}{\partial \hat{x}} = \frac{\alpha}{Pe}\frac{\partial^2 \hat{c}}{\partial \hat{y}^2} \quad 0 \le \hat{x} \le 1, \quad 0 \le \hat{y} \le 1 \tag{1}$$

$$\frac{\partial \hat{c}}{\partial \hat{y}}(\hat{x}, 0) = 0, \quad 0 \le \hat{x} \le 1 \tag{2}$$

$$\frac{\partial \hat{c}}{\partial \hat{y}}(\hat{x}, 1) = -Da, \quad 0 \le \hat{x} \le 1 \tag{3}$$

$$\hat{c}(0, \hat{y}) = 0, \quad 0 \le \hat{y} \le 1 \tag{4}$$

where $\hat{c}$ is the dimensionless concentration with respect inlet O_2 concentration, c_{in} ($\hat{c} = [c - c_{in}]/c_{in}$), and $\hat{x}$ and $\hat{y}$ are non-dimensionalized using the chamber height (H) and chamber length (L) according to $\hat{x} = x/L$ and $\hat{y} = y/H$. The Peclet number, a ratio of convective and diffusive transport, is defined as $Pe = u_m H/D$, where u_m is the mean velocity and D is oxygen diffusivity and $\alpha = L/H$.

The Damkohler number (Da) is the ratio of the oxygen uptake rate and diffusion rate and is a function of cell density and maximal oxygen uptake rate. The maximal oxygen uptake rate, V_{max}, in hepatocyte/fibroblast co-cultures may be primarily attributed to the highly metabolic hepatocyte fraction. However, the established model allows estimation of uptake characteristics of any culture system, including co-culture and fibroblast-only culture, by least-squares curve fitting. Experimentally determined V_{max} values and other model parameters used in calculation are listed in Table 1.

TABLE 1
Model Parameters

Parameter	Fibroblasts	Hepatocytes	Co-culture	Units
ρ, cell density	1.8×10^5	1.7×10^5	0.5×10^5	cells/cm^2
V_{max}, max. O_2 uptake	0.03	0.38[a]	0.4	nmol/s/10^6 cells
K_m, Michelis constant	1	5.6	5.6	mmHg
$Q_{gradient}$	0.06	0.6	0.3	ml/min
$Q_{critical}$ (<10 mmHg)	0.05	0.5	0.21	ml/min

[a]Rotem *et al.*, 1992.

RESULTS

Validation of Oxygen Gradients and Culture Viability

Perfusion of the flat-plate bioreactor (Fig. 1) was carried out with three different culture configurations: hepatocytes only, fibroblasts only, and hepatocyte/fibroblast co-culture. Under a fixed inlet gas mixture of 10% O_2/5% CO_2/85% N_2, oxygen measurements were acquired at the reactor outlet as a function of flow rate. In all cases, outlet oxygen partial pressure was found to decrease with decreasing flow rate with the greatest decrease at low flow rates (Fig. 2A). The range of flow rates at which oxygen levels become critical (<10 mmHg) depends on the intrinsic oxygen uptake of the cell as well as the cell density. The V_{max} of fibroblasts was experimentally determined by comparing measured outlet oxygen value to model predictions

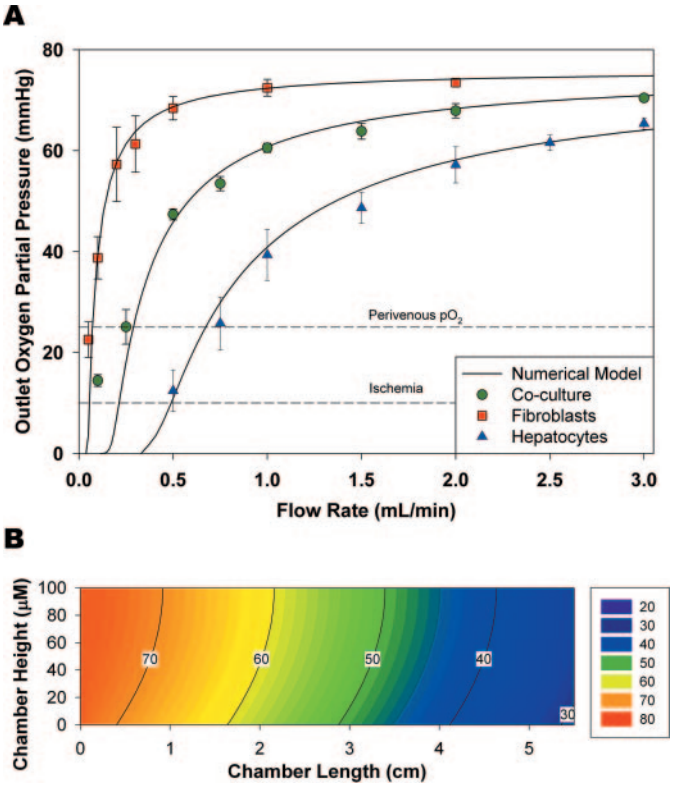

FIG. 2. Model and validation of oxygen gradients. (A) The outlet oxygen concentration was measured as a function of flow rate for three culture configurations; hepatocytes only, fibroblast only, and co-culture. Inlet pO_2 was kept constant during all experiments at 76 mmHg. Measured values represent the mean and SEM of three separate experiments. Numerical model predictions were determined using the following values: fibroblasts only (V_{max} = 0.025 nmol/s/10^6 fibs, ρ = 1.5×10^5 fibs/cm^2), hepatocytes only (V_{max} = 0.39 nmol/s/10^6 heps, ρ = 1.7×10^5 heps/cm^2), co-culture (V_{max} = 0.42 nmol/s/10^6 heps, ρ = 0.5×10^5 heps/cm^2) As indicated, typical perivenous oxygen tension of 25 mmHg indicates the desired outlet pO_2 for imposing a physiologic gradient on cultures and prevention of hypoxic injury may be avoided at pO_2 > 10 mmHg. (B) Two-dimensional contour plot of modeled oxygen profile in the medial cross section of the reactor. Results depict the cell surface gradient formed with inlet pO_2 of 76 mmHg and flow rate of 0.3 ml/min.

and minimizing the deviation by least-squares. As expected, the metabolic oxygen consumption by hepatocytes was an order of magnitude greater than fibroblasts alone resulting in an increase of the critical flow rate from 0.05 to 0.5 ml/min.

Having determined uptake kinetics of hepatocytes and fibroblasts independently, it was not known whether the oxygen consumption of a co-culture system would display linear correlation to the composite V_{max}. Hence, oxygen measurements were acquired for co-cultures as a function of flow rate. Experimental values were fit with the model by varying V_{max} and cell density parameters. It was determined that model predictions had stronger correlation when cell density was based on the hepatocyte density rather than total cell density. With this assumption, the experimentally derived V_{max} of 0.4 nmol/s/10^6 cells for hepatocytes in co-culture was comparable to the reported V_{max} for hepatocytes alone. With a validated model, we constructed a predicted oxygen concentration profile along the long axis of the reactor, which depicts formation of an oxygen gradient along the cell surface (Fig. 2B).

Viability of chamber co-cultures was assessed after 24, 48, and 72 h of perfusion at 0.3 ml/min, the flow rate at which outlet pO2 was equivalent to perivenous oxygen (~25–30 mmHg, Fig. 3). Total viability was greater than 85% in all regions of culture across all time points. Though a moderate trend of decreasing viability over time was observed, such changes were not statistically significant ($p > 0.05$). Cultures displayed characteristic polygonal morphology with functional bile canaliculi as shown by Calcein AM exocytosis.

Spatial Distribution of Induced CYP2B and CYP3A

To examine the role of oxygen gradients on drug induction, protein levels were assayed for CYP2B and CYP3A from discrete sections from the inlet region to the outlet region. These two enzymes are of interest because they exhibit regional expression patterns *in vivo* that are partially modulated by oxygen (Lindros, 1997). In all experiments, the perfusion reactor was operated with a constant inlet oxygen partial pressure of 76 mmHg and flow rate of 0.3 ml/min. Additional experimental variables involve supplementation of the media with PB (200 μM), a typical CYP2B inducer, DEX (5 μM), for CYP3A induction, and EGF (2 nM), a putative modulator of zonal heterogeneity.

Initially, day 5 cultures perfused with PB over 48 h showed dramatic expression of both CYP2B and CYP3A (Fig. 4A). Though expression of CYP2B was significant in all regions,

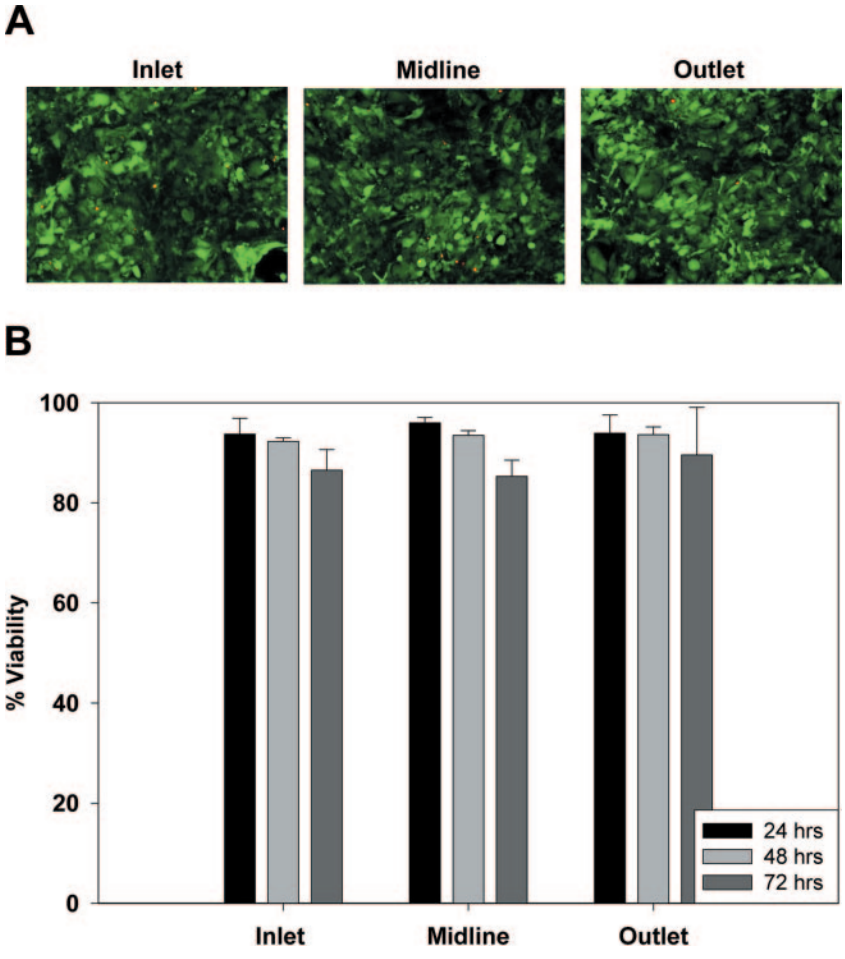

FIG. 3. Extended viability of bioreactor cultures. Chambers containing co-cultures were operated at 0.3 ml/min and 76 mm Hg inlet pO_2 for 24, 48, and 72 h. (A) Representative images from three regions after 72 h of perfusion are shown. (B) Viability was quantified for three fields from the inlet, midline, and outlet regions at each timepoint. Mean and SEM are shown.

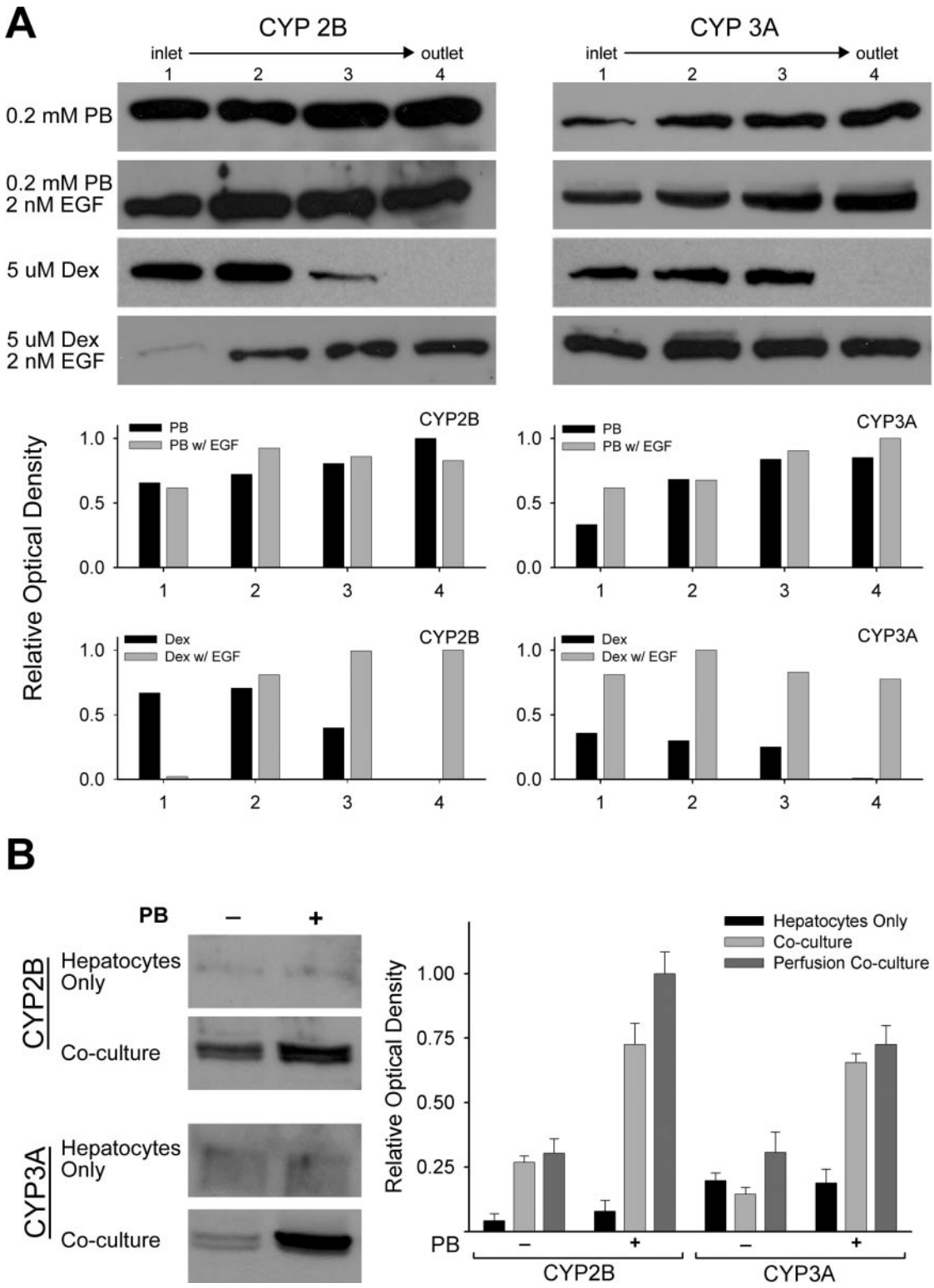

FIG. 4. Spatial expression of CYP2B and CYP3A. Western blot analysis was performed on whole cell lysates (20 μg protein) obtained from four separate regions along the length of the bioreactor. (A) Protein levels of CYP2B and CYP3A from day 5 cultures perfused for 48 h with combinations of PB, DEX, and EGF. Densiometric analysis of representative blots is shown to highlight spatial trend in protein level. (B) Similar analysis was performed on static hepatocyte only and co-cultures induced with PB for 48 h for comparison to bioreactor cultures. Both control and PB-treated blots are shown for CYP2B and CYP3A in static cultures with corresponding densiometric quantification. Bar graphs represent the mean and SEM for triplicate samples of static cultures and the mean of four regions from bioreactor cultures.

levels were highest in the lower-oxygen outlet regions. Similarly, CYP3A protein showed increasing expression from inlet to outlet. Based on previous studies that showed repression of PB-induced CYP2B expression by EGF, we added 2 nM EGF to the perfusion media (Allen and Bhatia, 2003; Kietzmann *et al*., 1999). At a dose of 200 μM PB, EGF did not significantly alter CYP2B levels along the length of the chamber though maximal levels were noted in the outlet regions. CYP3A levels in response to PB and EGF also showed little difference from PB-only perfusion displaying maximal expression at the outlet.

Experiments were also carried out to evaluate DEX as an inducer of CYPs in this perfusion system. DEX induced CYP2B to high levels that were localized to inlet regions of the culture. For CYP3A, induction was mostly uniform, but not detectable in the outlet region. When EGF was added to DEX-perfused cultures, a significant shift in CYP2B spatial distribution was noted from inlet regions to the outlet. CYP3A induction remained uniform in response to DEX and EGF, but was extended across all regions of the culture.

To compare expression to conventional static culture systems, chemical induction with PB was carried out on hepatocyte only and co-cultures (Fig. 4B). Basal expression of CYP2B and CYP3A in hepatocytes was scarcely detectable and lacked significant induction. In contrast, co-cultures showed higher constitutive CYP levels and were dramatically induced. Integrated optical density analysis showed that CYP levels were maximally induced in bioreactor cultures, suggesting that perfusion conditions further enhance cellular response to PB.

APAP Toxicity in Bioreactor Cultures

Acetaminophen (APAP) was evaluated for its acute toxic effect on hepatocyte cultures and co-cultures. Figure 5A shows a panel of images from full-length (~5.6 cm) bioreactor cultures (day 5) perfused with various concentrations of APAP for 24 h and then incubated with MTT. The presence and intensity of purple precipitate is proportional to cell viability. Of note is the dramatic decrease in staining from the inlet to the outlet region at a dose of 15 mM APAP as compared to uniform staining of the control and lack of signal from 20 mM.

For further quantification of regional variations in viability, bright-field images were acquired at low magnification (40×) along the length of the culture for measurement of mean optical density. The magnified portion of the 15 mM APAP condition in Figure 5B shows maximal toxicity in the outlet region, which decreased ~70% from the inlet region. Dose response to various concentrations of APAP was compared across culture models (Fig. 5C). Static culture of hepatocytes and co-cultures displayed a gradual decrease in viability with increasing APAP dose. Quantification of toxic dose response from the inlet and outlet regions was performed for comparison. Inlet regions showed similar trends to static cultures, but with a precipitous drop in viability at 20 mM APAP. Interestingly, in evaluating the TD_{50} (toxic dose to 50% of cells) of each culture system (Fig. 5D), the highest sensitivity to APAP dose was observed in the outlet region of perfusion cultures (13 mM) with decreasing toxicity in static co-culture (29 mM), and hepatocyte only culture (39 mM), respectively.

DISCUSSION

We have characterized a flat-plate hepatocyte bioreactor that effectively represents the spatial heterogeneity of liver microarchitecture. As a key parameter of the design, oxygen gradients were modeled and experimentally validated. A more thorough discussion of bioreactor design and the dynamics flow control and oxygenation were presented previously (Allen and Bhatia, 2003). Adaptation of the bioreactor to co-cultures of hepatocytes and fibroblasts, while allowing long-term viability under controlled oxygen gradients, required the revision of oxygen uptake rates, V_{max}, which were derived experimentally.

In Vitro *Models for Toxicological Evaluation*

Efforts to develop novel, *in vitro* toxicological testing platforms are ongoing both nationally and internationally (e.g., NICA; NIH). Historically, animal studies have formed the basis of toxicological evaluation but the benefit of intact *in vivo* response can be diminished by animal to animal variability and insensitive molecular analysis. Thus, fundamental to representative *in vitro* models of the liver is the use of primary hepatocytes. Cultures implementing variations of extracellular matrix environment and cell–cell interactions (homotypic and heterotypic) have been described, but engineered substrates allowing controlled interactions in hepatocyte/fibroblast co-cultures greatly augments liver-specific function and may provide long-term viability in toxicological studies (Bhatia *et al*., 1999; Dunn *et al*., 1991; Guguen-Guillouzo *et al*., 1983; Saito *et al*., 1992). In addition to primary culture, cell lines, such as HepG2 or HepLiu, provide an adequate *in vitro* liver model for many mechanistic studies of signal transduction, gene expression, metabolism, and toxicology, but their immortality render them somewhat dedifferentiated (Cederbaum *et al*., 2001; Fukaya *et al*., 2001; Liu *et al*., 1999). Isolated liver microsomes are a common system for studying the biochemical pathways of xenobiotic metabolism (Venkatakrishnan *et al*., 2002). While microsome-based models offer insight into molecular interactions of Phase I drug metabolism, they are an inadequate representation of the diversity of hepatocyte functions. Conversely, liver models that perfuse whole organs or wedge biopsies allow short-term studies of liver function at the cellular level, but offer limited molecular analysis (Burwen *et al*., 1982; Grosse-Siestrup *et al*., 2001). Liver slice systems, also applicable only to short-term metabolic and toxic studies, have, however, been evaluated using molecular assays (Drahushuk *et al*., 1996).

Several bioreactor systems have been proposed as novel *in vitro* liver models. A similar co-culture-based flat plate reactor evaluated the effects of oxygenation and fluid shear stress on

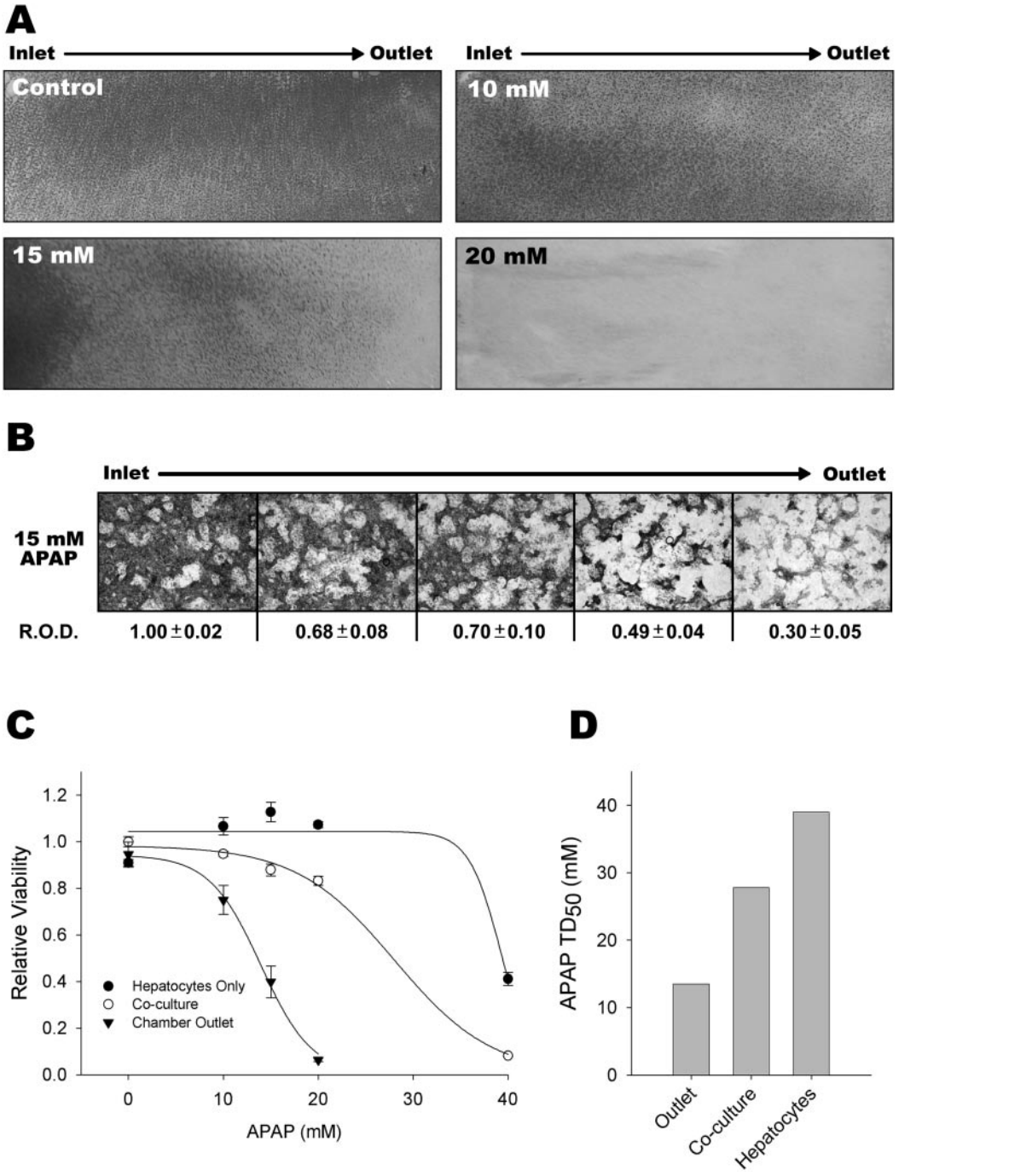

FIG. 5. Regional toxicity of APAP. (A) Representative perfusion of day 5 co-cultures were stained with MTT and photographed after 24 h perfusion with indicated concentrations of APAP. (B) Bright-field images of MTT-stained, perfused cultures were acquired from five regions along the length of the slide. Images from 15 mM APAP treatment are shown with relative optical density (R.O.D.) values representing mean and SEM ($n = 3$). (C) Comparison of 24 h dose response to APAP between hepatocytes (day 5), co-cultures (day 5), and regions of perfusion co-culture. Quantified MTT levels were normalized to respective control conditions. Mean and SEM are depicted ($n = 3$). (D) A three-paramter sigmoidal curve fit was applied to each dose reponse and the concentration at which viability was reduced to 50% (TD_{50}) was plotted.

bulk markers of hepatocyte function but was developed as a experimental liver support as evidenced by subsequent hepatic failure studies (Shito *et al*., 2003; Tilles *et al*., 2001). A multi-compartmental hollow-fiber based device which studied the metabolic and detoxification functions of liver co-cultures may not permit molecular studies or a unidirectional flow environment (Gerlach *et al*., 2003). Proposed as a platform for CYP3A4-mediated drug metabolism, a tumor derived cell

line was incorporated into a radial flow reactor (Iwahori *et al*., 2003). Finally, a perfused, microfabricated bioreactor containing preaggregated hepatocytes has undergone initial characterization and has shown improvement in cell viability and liver-specific function over conventional cultures (Powers *et al*., 2002). Though this three-dimensional system may lend itself well to some *in vitro* studies, it has not been evaluated or proposed as a toxicological model.

The current study employs a flat-plate bioreactor to impose physiologic gradients over phenotypically stable hepatocytes and evaluate spatial variations of CYP expression and toxicity. Among the current hepatocyte bioreactor configurations, including hollow-fiber and packed bed systems, flat-plate designs offer better control of cellular microenvironment and uniform perfusion. Additionally, the geometric advantages of flat-plate systems may allow for scaled-down, high-throughput screening or non-destructive evaluation of cellular responses to toxic insult.

Zonal Drug Metabolism and Toxicity In Vitro

Many members of the CYP superfamily responsible for phase I drug and steroid biotransformation are expressed in a zonal pattern *in vivo*. Among the determinants of the pericentral localization of CYPs under both normal and induced conditions are gradients of oxygen, nutrients, and hormones (Lindros, 1997). Recapitulation of these dynamic gradients in bioreactor cultures resulted in spatial distributions of both CYP2B and CYP3A that mimic those found *in vivo*. Additionally, CYP induction was potentiated by the perfusion microenvironment of the reactor as shown by the dramatic increase in protein levels over static cultures in response to 200 μM PB (Fig. 4B). Previous studies demonstrated that the repressive effects of EGF on PB induction are modulated by oxygen (Allen and Bhatia, 2003; Kietzmann *et al*., 1999). Addition of EGF with PB in the current study did not significantly alter the spatial CYP2B pattern, but in conjunction with DEX, EGF shifted maximal CYP2B expression from the inlet to the outlet. This shifting effect, also noted to a lesser extent in CYP3A expression, may be due the formation of EGF gradients, thus demonstrating how dynamic gradients of growth factors and hormones regulate CYP zonation. Finally, though overlapping CYP2B and CYP3A induction by PB and DEX is likely mediated by nuclear hormone receptors such as constitutive androstane and pregnane X, the mechanism by which oxygen availability and hormones can modulate these pathways remains to be elucidated (Corcos and Lagadic-Gossmann, 2001).

Toxic dose-response in hepatocyte co-culture has not been previously reported, but maximal toxic dose of 40 mM APAP is comparable to other studies in primary rat hepatocytes, which appear to be more resistant to APAP toxicity (Lewerenz *et al*., 2003). Though it is difficult to extrapolate to *in vivo* dose response, moderate toxicity at 20 mM in our static culture is not significantly higher than an assumed distribution to the extracellular compartment (13–21 mM) resulting from an ip injection of 500–800 mg APAP/kg (Zhang *et al*., 2002). Additionally, perfusion of APAP resulted in a shift in the dose response such that 20 mM was completely toxic in bioreactor cultures as compared to 40 mM in static cultures. Furthermore, perfusion cultures at 15 mM demonstrated a toxicity pattern similar to the centrilobular localization seen *in vivo*. This *in vitro* zonal toxicity provides insight into the deleterious effects of APAP and the factors that contribute to spatial toxicity which would not be observed in conventional culture models.

The proposed mechanism of APAP hepatotoxicity involves the formation of a reactive intermediate, NAPQI, which initiates free-radial damage of intracellular structures (McClain *et al*., 1999). Toxic effects in this study are likely due to the depletion of glutathione, which provides protective inactivation of NAPQI. Though pericentral localization of APAP toxicity *in vivo* has been attributed to local expression of CYP isoenzymes 2E1 and 3A (Anundi *et al*., 1993; Sinclair *et al*., 1998), reduced oxygen availability in centrilobular regions may also contribute by depleting ATP and glutathione, or increasing damage by reactive species (Jaeschke *et al*., 2002). A combination of these factors likely resulted in the regional toxicity observed in reactor cultures under dynamic oxygen gradients. Demonstration of zonal toxicity *in vitro* allows decoupling of the effects of CYP bioactivation and glutathione levels on acute APAP toxicity. Furthermore, this system may allow elucidation of the actions of various clinically important compounds such as ethanol or N-acetyl-cysteine and their respective exacerbating or protective effects on APAP toxicity (Zhao *et al*., 1998, 2002).

In conclusion, we have evaluated a perfusion-based hepatocyte co-culture system as platform to study CYP induction, drug metabolism, and resultant toxicity. As demonstrated by perivenous-like CYP expression and toxicity patterns, this culture model represents a novel means of exploring liver zonation and its physiologic implications. In addition to basic applications in drug screening and toxicology, this biomimetic system may provide a controllable environment to investigate the spatial and temporal dynamics of hepatotoxicity. For example, pre-induction of cultures with low concentrations of EtOH followed by APAP dosing may offer insight into the susceptibility to APAP toxicity with alcohol consumption. Further adaptation of this system to other co-culture models with liver-derived non-parenchymal cells may recapitulate crosstalk that has been implicated in the pathogenesis of chemically induced hepatic dysfunction.

ACKNOWLEDGMENTS

The authors would like to thank Jennifer Felix for her technical contributions. Funding for this work was provided by Whitaker Foundation, Packard Foundation, NIH DK065152, and NIH DK56966.

REFERENCES

Allen, J. W., and Bhatia, S. N. (2003). Formation of steady-state oxygen gradients *in vitro*: Application to liver zonation. *Biotechnol. Bioeng.* **82,** 253–262.

Anundi, I., Lahteenmaki, T., Rundgren, M., Moldeus, P., and Lindros, K. O. (1993). Zonation of acetaminophen metabolism and cytochrome P450 2E1-mediated toxicity studied in isolated periportal and perivenous hepatocytes. *Biochem. Pharmacol.* **45,** 1251–1259.

Baron, J., Redick, J. A., and Guengerich, F. P. (1982). Effects of 3-methylcholanthrene, beta-naphthoflavone, and phenobarbital on the 3-methylcholanthrene-inducible isozyme of cytochrome P-450 within centrilobular, midzonal, and periportal hepatocytes. *J. Biol. Chem.* **257,** 953–957.

Bars, R. G., Bell, D. R., Elcombe, C. R., Oinonen, T., Jalava, T., and Lindros, K. O. (1992). Zone-specific inducibility of cytochrome P450 2B1/2 is retained in isolated perivenous hepatocytes. *Biochem. J.* **282**(Pt. 3), 635–638.

Bhatia, S. N., Balis, U. J., Yarmush, M. L., and Toner, M. (1999). Effect of cell-cell interactions in preservation of cellular phenotype: Cocultivation of hepatocytes and nonparenchymal cells. *FASEB J.* **13,** 1883–1900.

Burwen, S. J., Jones, A. L., Goldman, I. S., Way, L. W., and Dejbakhsh, S. (1982). The perfused human liver wedge biopsy: A new *in vitro* model for morphological and functional studies. *Hepatology* **2,** 426–432.

Cederbaum, A. I., Wu, D., Mari, M., and Bai, J. (2001). CYP2E1-dependent toxicity and oxidative stress in HepG2 cells. *Free Radic. Biol. Med.* **31,** 1539–1543.

Corcos, L., and Lagadic-Gossmann, D. (2001). Gene induction by Phenobarbital: An update on an old question that receives key novel answers. *Pharmacol. Toxicol.* **89,** 113–122.

Drahushuk, A. T., McGarrigle, B. P., Tai, H. L., Kitareewan, S., Goldstein, J. A., and Olson, J. R. (1996). Validation of precision-cut liver slices in dynamic organ culture as an *in vitro* model for studying CYP1A1 and CYP1A2 induction. *Toxicol. Appl. Pharmacol.* **140,** 393–403.

Dunn, J. C., Tompkins, R. G., and Yarmush, M. L. (1991). Long-term *in vitro* function of adult hepatocytes in a collagen sandwich configuration. *Biotechnol. Prog.* **7,** 237–245.

Fukaya, K., Asahi, S., Nagamori, S., Sakaguchi, M., Gao, C., Miyazaki, M., and Namba, M. (2001). Establishment of a human hepatocyte line (OUMS-29) having CYP 1A1 and 1A2 activities from fetal liver tissue by transfection of SV40 LT. *In Vitro Cell Dev. Biol. Anim.* **37,** 266–269.

Gerlach, J. C., Mutig, K., Sauer, I. M., Schrade, P., Efimova, E., Mieder, T., Naumann, G., Grunwald, A., Pless, G., Mas, A., Bachmann, S., Neuhaus, P., and Zeilinger, K. (2003). Use of primary human liver cells originating from discarded grafts in a bioreactor for liver support therapy and the prospects of culturing adult liver stem cells in bioreactors: A morphologic study. *Transplantation* **76,** 781–786.

Giffin, B. F., Drake, R. L., Morris, R. E., and Cardell, R. R. (1993). Hepatic lobular patterns of phosphoenolpyruvate carboxykinase, glycogen synthase, and glycogen phosphorylase in fasted and fed rats. *J. Histochem. Cytochem.* **41,** 1849–1862.

Grosse-Siestrup, C., Nagel, S., Unger, V., Meissler, M., Pfeffer, J., Fischer, A., and Groneberg, D. (2001). The isolated perfused liver. A new model using autologous blood and porcine slaughterhouse organs. *J. Pharmacol. Toxicol. Methods* **46,** 163.

Guguen-Guillouzo, C., Clément, B., Baffet, G., Beaumont, C., Morel-Chany, E., Glaise, D., and Guillouzo, A. (1983). Maintenance and reversibility of active albumin secretion by adult rat hepatocytes co-cultured with another liver epithelial cell type. *Exp. Cell Res.* **143,** 47–54.

Haussinger, D. (1983). Hepatocyte heterogeneity in glutamine and ammonia metabolism and the role of an intercellular glutamine cycle during ureogenesis in perfused rat liver. *Eur. J. Biochem.* **133,** 269–275.

Iwahori, T., Matsuura, T., Maehashi, H., Sugo, K., Saito, M., Hosokawa, M., Chiba, K., Masaki, T., Aizaki, H., Ohkawa, K., and Suzuki, T. (2003). CYP3A4 inducible model for *in vitro* analysis of human drug metabolism using a bioartificial liver. *Hepatology* **37,** 665–673.

Jaeschke, H., Gores, G. J., Cederbaum, A. I., Hinson, J. A., Pessayre, D., and Lemasters, J. J. (2002). Mechanisms of hepatotoxicity. *Toxicol. Sci.* **65,** 166–176.

Jungermann, K., and Kietzmann, T. (1996). Zonation of parenchymal and nonparenchymal metabolism in liver. *Annu. Rev. Nutr.* **16,** 179–203.

Jungermann, K., and Kietzmann, T. (2000). Oxygen: Modulator of metabolic zonation and disease of the liver. *Hepatology* **31,** 255–260.

Jungermann, K., and Thurman, R. G. (1992). Hepatocyte heterogeneity in the metabolism of carbohydrates. *Enzyme* **46,** 33–58.

Kietzmann, T., Hirsch-Ernst, K. I., Kahl, G. F., and Jungermann, K. (1999). Mimicry in primary rat hepatocyte cultures of the *in vivo* perivenous induction by phenobarbital of cytochrome P-450 2B1 mRNA: Role of epidermal growth factor and perivenous oxygen tension. *Mol. Pharmacol.* **56,** 46–53.

Lewerenz, V., Hanelt, S., Nastevska, C., El-Bahay, C., Rohrdanz, E., and Kahl, R. (2003). Antioxidants protect primary rat hepatocyte cultures against acetaminophen-induced DNA strand breaks but not against acetaminophen-induced cytotoxicity. *Toxicology* **191,** 179–87.

Lindros, K. O. (1997). Zonation of cytochrome P450 expression, drug metabolism and toxicity in liver. *Gen. Pharmacol.* **28,** 191–196.

Liu, J., Pan, J., Naik, S., Santangini, H., Trenkler, D., Thompson, N., Rifai, A., Chowdhury, J. R., and Jauregui, H. O. (1999). Characterization and evaluation of detoxification functions of a nontumorigenic immortalized porcine hepatocyte cell line (HepLiu). *Cell Transplant.* **8,** 219–232.

McClain, C. J., Price, S., Barve, S., Devalarja, R., and Shedlofsky, S. (1999). Acetaminophen hepatotoxicity: An update. *Curr. Gastroenterol. Rep.* **1,** 42–49.

NICA (Nordic Information Centre for Alternative Method). Multicentre Evaluation of *In Vitro* Cytotoxicity, Accessed 8/2004, http://www.cctoxconsulting.a.se/meic.htm.

NIH. National Toxicology Program, Accessed 8/2004, http://ntp-server.niehs.nih.gov/.

Powers, M. J., Domansky, K., Kaazempur-Mofrad, M. R., Kalezi, A., Capitano, A., Upadhyaya, A., Kurzawski, P., Wack, K. E., Stolz, D. B., Kamm, R., and Griffith, L. G. (2002). A microfabricated array bioreactor for perfused 3D liver culture. *Biotechnol. Bioeng.* **78,** 257–269.

Rotem, A., Toner, M., Tompkins, R. G., and Yarmush, M. L. (1992). Oxygen uptake rates in cultured rat hepatocytes. *Biotechnol. Bioeng.* **40,** 1286–1291.

Saito, S., Sakagami, K., Matsuno, T., Tanakaya, K., Takaishi, Y., and Orita, K. (1992). Long-term survival and proliferation of spheroidal aggregate cultured hepatocytes transplanted into the rat spleen. *Transplant Proc.* **24,** 1520–1521.

Seglen, P. O. (1976). Preparation of isolated rat liver cells. *Methods Cell. Biol.* **13,** 29–83.

Shito, M., Tilles, A. W., Tompkins, R. G., Yarmush, M. L., and Toner, M. (2003). Efficacy of an extracorporeal flat-plate bioartificial liver in treating fulminant hepatic failure. *J. Surg. Res.* **111,** 53–62.

Sinclair, J., Jeffery, E., Wrighton, S., Kostrubsky, V., Szakacs, J., Wood, S., and Sinclair, P. (1998). Alcohol-mediated increases in acetaminophen hepatotoxicity: Role of CYP2E and CYP3A. *Biochem. Pharmacol.* **55,** 1557–1565.

Teutsch, H. F. (1986). A new sample isolation procedure for microchemical analysis of functional liver cell heterogeneity. *J. Histochem. Cytochem.* **34,** 263–267.

Tilles, A. W., Baskaran, H., Roy, P., Yarmush, M. L., and Toner, M. (2001). Effects of oxygenation and flow on the viability and function of rat hepatocytes cocultured in a microchannel flat-plate bioreactor. *Biotechnol. Bioeng.* **V73,** 379–389.

Venkatakrishnan, K., Von Moltke, L. L., and Greenblatt, D. J. (2002). Evaluation of SupermixTM as an *in vitro* model of human liver microsomal drug metabolism. *Biopharm. Drug Dispos.* **23,** 183–190.

Zhang, J., Huang, W., Chua, S. S., Wei, P., and Moore, D. D. (2002). Modulation of acetaminophen-induced hepatotoxicity by the xenobiotic receptor CAR. *Science* **298,** 422–424.

Zhao, C., Sheryl, D., and Zhou, Y. X. (1998). Effects of combined use of diallyl disulfide and N-acetyl-cysteine on acetaminophen hepatotoxicity in beta-naphthoflavone pretreated mice. *World J. Gastroenterol.* **4,** 112–116.

Zhao, P., Kalhorn, T. F., and Slattery, J. T. (2002). Selective mitochondrial glutathione depletion by ethanol enhances acetaminophen toxicity in rat liver. *Hepatology* **36,** 326–335.